Effect of temperature- and composition-dependent deep level energies on electrical compensation: Experiment and model of the $Cd_{1-x}Zn_xTe$ system

Michael Prokesch* and Csaba Szeles
eV PRODUCTS a division of II-VI Incorporated, 373 Saxonburg Boulevard, Saxonburg, Pennsylvania 16056, USA
(Received 24 January 2007; revised manuscript received 2 April 2007; published 13 June 2007)

The effect of temperature and composition dependences of deep level ionization energies in semi-insulating compound semiconductors is investigated and illustrated in the example of the ternary $Cd_{1-x}Zn_xTe$ system. Those dependences are determined by the behavior of the band extrema in an absolute energy scale and the actual nature of a particular defect, which controls its relation to the host crystal states. Examples for the interpretation of experimental temperature and composition dependences of critical charge transport parameters are given.

DOI: 10.1103/PhysRevB.75.245204 PACS number(s): 71.55.Gs, 07.85.Fv

I. INTRODUCTION

Despite significant commercial success and nearly half a century of research in the field of wide-band-gap compound semiconductors, fundamental understanding of electrical compensation and charge transport controlling defects and associated electronic processes in this material class is not adequate.[1,2] A general problem is the extremely limited availability of reliable and relevant direct defect data, which is caused by either technical or even fundamental limitations. This is especially true for deep energy levels corresponding to point defects of completely different nature and properties (e.g., foreign impurities like transition metals, native defects, defect complexes, etc.) that can control the semiconductor's properties already at concentrations well below the detection limits of standard spectroscopic techniques. In semi-insulating semiconductors, the dominating role of these defects in the control of electrical compensation leads to some—often overlooked—implications that can significantly complicate the modeling of electrical and charge transport properties. This concerns the interpretation of experimental temperature and composition dependences of critical charge transport parameters, which we will try to illustrate in this work in the example of semi-insulating (SI) CdZnTe, a ternary compound of special importance for applications in room-temperature photon and particle detection.[3]

II. DEEP LEVEL COMPENSATION

Electrically compensated $Cd_{1-x}Zn_xTe$, as used for radiation detector fabrication, can be obtained with a room-temperature (RT) resistivity of several $10^{10}\ \Omega$ cm. This requires "majority" carrier concentrations below $10^6\ cm^{-3}$. The theoretical maximum resistivity ρ_{max} is reached when the drift-mobility-concentration products of free electrons and holes ($\mu_n n$ and $\mu_p p$) are equal, which gives

$$\rho_{max} = \frac{1}{2qn_i\sqrt{\mu_n\mu_p}}, \tag{1}$$

where q is the elementary charge and $n_i=\sqrt{np}$ the intrinsic carrier concentration. Equation (1) follows directly from $\rho=1/q(\mu_n n+\mu_p p)$ for $\mu_n n=\mu_p p$. Using the parameters from Ref. 4 at 296 K and 10% Zn—which is the technologically most interesting and commercially readily available $Cd_{1-x}Zn_xTe$ composition—one obtains $\rho_{max}\sim 1\times 10^{11}\ \Omega$ cm. At this point, the conduction type would be indefinite and the hole concentration $\hat{p}=n_i\sqrt{\mu_n/\mu_p}\sim 6\times 10^5\ cm^{-3}$, which is about 20 times higher than the corresponding electron concentration (inverse mobility ratio). In practice, semi-insulating CZT will have a slightly lower RT resistivity and be either slightly *n*-type or slightly *p*-type.

In any event, such low free-carrier concentrations cannot be achieved by matching of shallow level defect concentrations by any technologically practical means but requires the contribution of deep (close to midgap) levels. We suggest the following formulation as a general condition to obtain SI semiconductor crystals by deep level (DL) compensation:

$$\sum_i N_{A\_i}^{shallow} \le \sum_j N_{D\_j}^{shallow} + \sum_k N_{D\_k}^{deep},$$

$$\sum_j N_{D\_j}^{shallow} \le \sum_i N_{A\_i}^{shallow} + \sum_l N_{A\_l}^{deep}, \tag{2}$$

which simply means that the total concentration of all shallow acceptors, $N_{A\_i}^{shallow}$, must be smaller than the total concentration of all shallow and deep donors, $N_{D\_j}^{shallow}$ and $N_{D\_k}^{deep}$. At the same time, the total concentration of the shallow donors, $N_{D\_j}^{shallow}$, has to be smaller than the total concentration of all acceptors, $N_{A\_i}^{shallow}$ and $N_{A\_l}^{deep}$. Condition (2) remains fully valid if defects with multiple charge states are individually indexed for each of their energy levels. Note that the formulation given in Ref. 5 is a special scenario within this condition. It is to be pointed out, however, that a simple comparison of the total numbers of donors and acceptors does not necessarily predict the conduction type of SI material as this also depends on the actual DL ionization energies.

III. BAND EDGES IN ABSOLUTE ENERGY SCALE

For many modeling purposes knowledge of the temperature (T) and composition (mole fraction x) dependence of the band gap $E_G(T,x)$ is sufficient. This dependence is experimentally accessible by, e.g., photoluminescence and reflec-

tance or optical transmission measurements and can be expressed as an approximating matrix:

$$E_G(T,x) = E_G(0K,CdTe) + a_1 x + a_2 x^2 - \frac{a_3 T^2}{a_4 + T}, \quad (3)$$

where the a_i are experimental or adjusted parameters.[4]

However, a more comprehensive and relevant modeling of the electrical compensation and charge transport properties requires knowledge of the temperature and composition dependences of the band extrema and relevant defect levels with respect to a host-crystal-independent reference level—i.e., on an absolute energy scale.[6] Though some data on band offsets in heterostructures are available (e.g., Ref. 7 and references therein), there is only limited experimental information about the temperature and composition behavior of band edges in individual bulk compounds. An often overlooked problem is that the energy levels of certain point defects may or may not closely follow either of the band-edge dependences $E_C(T,x)$ or $E_V(T,x)$, which can lead to significantly different temperature and/or concentration dependences of the relevant ionization energies. This depends on the nature of the respective defect and with which band a certain energy level communicates. This is of critical importance when spectroscopic energy data of deep level defects, which are usually obtained by methods like photo electron paramagnetic resonance (photo-EPR) or optically detected magnetic resonance (ODMR) at very low temperatures (e.g., Refs. 8 and 9) are used for the modeling of RT of even high-temperature defect equilibria (at crystal growth, ingot cooldown, or annealing temperature). Defects that play an important role in charge trapping at RT may not even have an energy level in the forbidden gap at crystal growth temperature. This effect has to be also considered in the analysis of temperature-dependent high-precision resistivity measurements of SI material (see Sec. V).

Our approach to this problem is to define the valance-band edge of the pure binary CdTe at 0 K as the reference energy (e.g., zero) and add a linear temperature correction:

$$E_V(T,x) = E_V(0K,CdTe) + \alpha_T T. \quad (4)$$

The linear temperature coefficient $\alpha_T = -10^{-4}$ eV/K has been taken from a theoretical work.[10]

On the other hand, following common anion reasoning,[11] the composition-related valence-band offset should be rather small in the CdTe-ZnTe system. Though x-ray photoelectron spectroscopic results on CdTe-ZnTe heterostructures may indicate a small offset (e.g., ~0.1 eV in Ref. 12), those strain-affected interface data may not be representative of bulk binary crystals, possible effects of interface dipoles on band lineups aside.[13] Furthermore, this small valence-band offset is in the error range of zero-strain offset estimates.[14] In addition, the interesting Zn concentration range in the $Cd_{1-x}Zn_xTe$ system—relevant for detector applications—is typically (5–15)%, so that even a (hypothetical) 0.1 eV offset between the two binaries would translate to only a ~10 meV shift of the absolute valence-band maximum position at a given temperature. This is small compared to the ~47 meV RT band-gap variation over the same composition range, so that the complete omission of the Zn concentration dependence, which would add a term to Eq. (4) can be justified.

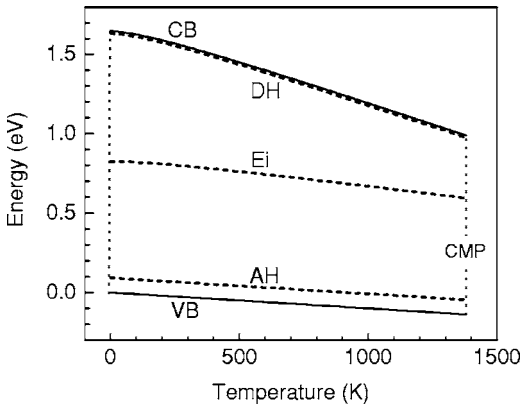

FIG. 1. Theoretical temperature dependences of the fundamental band edges (CB and VB) according to Eqs. (3)–(5), hydrogenic donor and acceptor levels (DH and AH) according to Eq. (6), and intrinsic Fermi level (Ei) according to Eq. (7) for $Cd_{0.9}Zn_{0.1}Te$ in an absolute energy scale. CMP: congruent melting point.

Eventually, with Eqs. (3) and (4), the conduction-band edge in absolute energy scale is defined as

$$E_C(T,x) = E_V(T,x) + E_G(T,x). \quad (5)$$

IV. TEMPERATURE DEPENDENCE OF IONIZATION ENERGIES

A. Delocalized, hydrogenic defects

Delocalized, hydrogenic donor and acceptor states are made of the respective band states and therefore, can be expected to energetically follow the temperature and composition dependences of the band extrema $E_C(T,x)$ or $E_V(T,x)$. The ionization energies of those (usually shallow) defects are therefore temperature independent, in a first approximation. This is illustrated in Fig. 1 in an absolute energy scale. The ionization energy of an ideal hydrogenic level can be estimated by

$$E_H^{eff} \sim \frac{m^*}{m_0 \varepsilon_r} \times 13.6 \text{ eV} - E_{pot}, \quad (6)$$

where m^*/m_0 is the relative carrier effective mass in the respective band and ε_r is the static dielectric constant of the semiconductor, which we assume to be temperature independent in a first approximation. E_{pot} describes the lowering of the effective ionization energy in case of high net-doping concentrations (e.g., Ref. 15). However, E_{pot} should be practically zero in semi-insulating material.

Also shown in Fig. 1 is the intrinsic Fermi level, which is, per definition,

$$E_I(T,x) = E_V(T,x) + \frac{E_G(T,x)}{2} - \frac{3}{4} k_B T \ln\left(\frac{m_e^*}{m_h^*}\right), \quad (7)$$

where k_B is the Boltzmann constant and m_e^* and m_h^* are the electron and hole effective masses. The intrinsic Fermi level

is at midgap for $T=0$ but—due to the smaller effective mass of the electrons—deviates to the upper half of the forbidden gap as the temperature increases, though it moves down in absolute energy.

B. Transition metals

Some foreign impurities like transition metals (TMs) generate highly localized states with energy levels that are generally independent of the host crystal and may even serve as a guide to predict band-gap discontinuities in semiconductor heterojunctions.[6] Consequently, they are not expected to closely follow any $E_C(T,x)$ or $E_V(T,x)$ trends. Instead, we assume them to be temperature independent on an absolute energy scale; i.e., their ionization energies will critically depend on the actual energy position of the respective band edge at a given temperature.

C. Native defects

We are not aware of any detailed theoretical investigation of the temperature and compositional dependences of the energy levels of native defects, so we apply the following reasoning. Native defects (NDs) are built up entirely from host atom orbitals, which also generate the band states. The assumption that, e.g., the cation vacancy and Te antisite (Te_{Cd}) states in CdZnTe are primarily built up by Te orbitals would imply at least some coupling to the valence band(s), or, in general, defects that are built up from anion orbitals are assumed to follow the valence-band dependences $E_V(T,x)$. In this case, their ionization energies change with the temperature (and composition of the ternary compound) if the associated energy levels communicate with the conduction band (donor states) but are rather temperature independent if they generate acceptor states. The opposite is applied to defects built up by cation orbitals.

Though this type of behavior seems to be suggested by some experimental data on certain native defects in II-VI compounds,[16] there may be additional contributions from the whole Brillouin zone, which can be expected to blur the "trends" by producing at least some degree of localization of the wave functions of the corresponding states,[17] so that, in practice, a perfect temperature independence of the ionization energy should never be expected. Also, a closer look at the ways some of the data, collected in Ref. 16, were actually obtained or derived may leave at least some question marks.[18]

Note that the here mentioned defects are purely hypothetical examples at this point; e.g., the Te_{Cd} antisite is a popular theoretical candidate to participate in the compensation in some form.[19] However, we are not aware of any direct spectroscopic evidence of the existence of isolated antisite defects in any of the II-VI compounds (e.g., by means of EPR, ODMR, etc.).

Isolated interstitial defects—if they were stable at RT—could exist in two different configurations in the zinc-blende lattice and may even undergo cyclic conversions between the tetrahedral sites surrounded by four Cd/Zn atoms and those surrounded by four Te atoms.[20] Direct detection of this defect type, however, has been only successful after generation of Frenkel pairs by particle irradiation at very low temperatures and even the farthest separated pairs annihilated well below RT by migration of the interstitial.[21] It is important to note that in those experiments a metastable nonequilibrium has been produced and the crystal will minimize its total energy as soon as thermally possible. However, if the interstitial defect is generated as part of a self-compensation process (e.g., in response to impurity doping at high temperatures), the existence of RT stable point-defect complexes involving interstitial defects cannot be excluded.

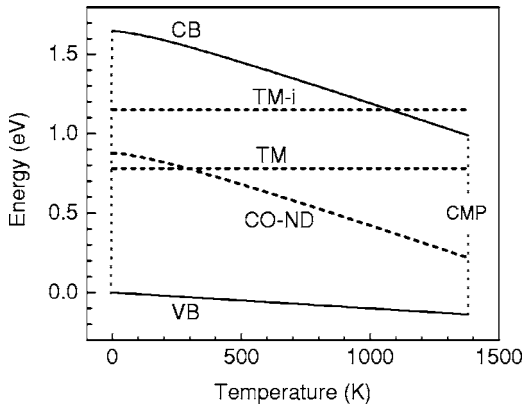

FIG. 2. Theoretical temperature dependence of the fundamental band edges (CB and VB) according to Eqs. (3)–(5), idealized transition metal levels (TM-i and TM) as explained in the text, and a "cation-orbital native defect" (CO-ND) in $Cd_{0.9}Zn_{0.1}Te$ in an absolute energy scale. CMP: congruent melting point.

Point-defect complexes should show a behavior somewhere in between the extreme cases outlined above. As an example, *A* center-like complexes (cation vacancy bound to a donor impurity) may behave slightly different dependent on whether the participating donor state is delocalized or arises from a transition-metal-like impurity. Moreover, the influence of the actual donor on the electron distribution of the *A* center should be less significant if the donor occupies a cation site like most group-III elements and transition metals in II-VI materials, because in this case the donor represents only the next-nearest neighbor of the dominating vacancy defect. Sometimes, simple configurational considerations can already explain the trend of differences in measured *A* center ionization energies with respect to the "undisturbed" vacancy defect.[9] In general, the distortion of the vacancy's electron distribution by the donor atom can be expected to be rather small. In fact, reported *A*-center energies closely follow the isolated vacancy,[16] of course ignoring possible experimental uncertainties or misinterpretations.

Figure 2 compares the situations for a transition-metal-like impurity (TM) and an idealized native defect built of cation orbitals (ND). The two energy levels coincide at RT, and both could serve to pin the Fermi level at midgap but they behave very different when the temperature changes. The change in the ionization energies will be strongest if the TM is a donor and the ND is an acceptor. On the other hand, if the TM impurity is an acceptor, it would still show some temperature dependence, whereas a native donor's ionization energy would be temperature independent. Also shown in

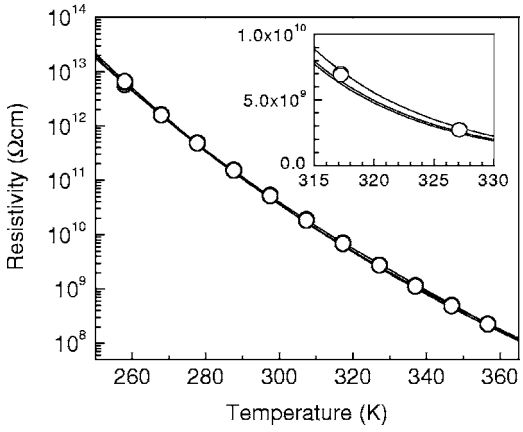

FIG. 3. Temperature-dependent bulk resistivity measurement on CdZnTe (13.8% Zn). Open circles: experimental data. Straight lines: scenario fits (1)–(3); see Sec. V for details. The linear-scale inset shows the very small differences between the fits in a 15 K temperature window.

Fig. 2 is an intermediate TM level (TM-i)—i.e., a level that could significantly influence the detector properties at RT by contributing detrapping to the charge transport with time constants in the order of the experimental time scale (typically the transit time of the carriers in the detector device). However, this energy level would only move into the forbidden gap at some point during crystal cooldown from the growth temperature. At high temperature the defect level is in the conduction band. (The right temperature edge in Fig. 2 corresponds to the congruent melting point of $Cd_{0.9}Zn_{0.1}Te$.)

V. TEMPERATURE-DEPENDENT RESISTIVITY

Traditional four-probe techniques (e.g., van der Pauw measurements of resistivity and Hall coefficient) are often not applicable to SI material because of significant surface contributions, so that a guarded low-bias two-probe measurement sometimes represents the only way to obtain reliable bulk resistivity data.[4]

Figure 3 shows the result of a temperature-dependent resistivity measurement on an SI-CdZnTe crystal sample. The bulk resistivity changes by almost five orders of magnitude in the (258–358) K temperature range.

Even though it was straight forward to incorporate a drift mobility correction in our model routines, this was not a critical contribution. The actual temperature dependence of the carrier mobilities in SI material does not significantly affect the $\rho(T)$ slope, so that a pure $\rho(T)$ measurement directly yields information about the temperature dependence of the free-carrier concentrations.

The calculation of the free-carrier and ionized-defect concentrations is based on the solution of the charge-neutrality condition, which may be expressed as

$$n + k_m \sum_m N_{A\_m}^{(-k_m)} = p + k_n \sum_n N_{D\_n}^{(+k_n)}; \tag{8}$$

i.e., the number of all negative charges (ionized acceptor states, N_{A_m}, and free electrons, n) has to equal the number of all positive charges (ionized donor states, N_{D_n}, and free holes, p). The k_m and k_n indicate the actual charge states $(1,2,\ldots)$. The individual concentrations of each species are given by the Fermi statistics. As an example, the ionized concentration $N_{D\_j}^{+}$ of a single donor j with total concentration N_{D_j} and degeneracy g_{D_j} is entirely determined by the energy difference between its 0/+ transition level E_{D_j} and the Fermi energy E_F:

$$\frac{N_{D\_j}^{+}}{N_{D\_j}}(T,x) = \frac{1}{1 + g_{D\_j} \exp\left(-\dfrac{E_{D\_j}(T,x) - E_F(T,x)}{k_B T}\right)}, \tag{9}$$

where k_B is the Boltzmann constant and T is the temperature. (Note the general temperature and composition dependence of the dopant level.) Similar equations apply for ionized acceptors. The degeneracy factors, however, may be different for donors and acceptors depending on the band structure of a given semiconductor.[22] Once the neutrality equation is solved for E_F, all individual ionized fractions including the free-carrier concentrations can be obtained. The free-electron concentration n is given by

$$\frac{n}{N_C}(T,x) = \exp\left(-\frac{E_C(T,x) - E_F(T,x)}{k_B T}\right), \tag{10}$$

where E_C is the conduction-band minimum energy according to Eqs. (3)–(5) and N_C is the conduction-band density of states. Each term of the neutrality equation (8)—including the free-carrier concentration terms—contributes one order; i.e., for instance, a three-level model corresponds to a fifth-order polynomial equation in E_F, though in many practical cases all shallow donors and acceptors can be summarized in a single net shallow doping term, comprising only the difference of the total shallow acceptor and shallow donor concentrations $(N_{AS}^{tot} - N_{DS}^{tot})$, which reduces the overall numerical effort.

In presence of a multitude of deep levels, the $\rho(T)$ dependence may be governed by more than one defect species, and if no additional experimental information is available, the same experimental $\rho(T)$ dependence can be fitted by an infinite variety of scenarios involving different ionization energies. Here, we want to show that already in the most simple (although very important practical scenario) case of one dominating deep level species, the obtained ionization energy will depend on the actual nature of the defect (e.g., TM or ND). Furthermore, a $\rho(T)$ measurement does not provide any information on the donor or acceptor nature of the deep level; i.e., the same data can be fitted by either a deep donor or deep acceptor model. In order to resolve this ambiguity, additional experimental data, such as majority-carrier-type measurements, have to be obtained and used within one consistent defect model.

On the other hand, the $\rho(T)$ measurement is extremely sensitive to even small (<0.01 eV) changes in the (effective) deep level ionization energies in compensated SI material and, hence, provides a sensitive tool to study those: In Fig. 3, the experimental $\rho(T)$ data are fitted with different scenarios where a net concentration of shallow donors and acceptors is

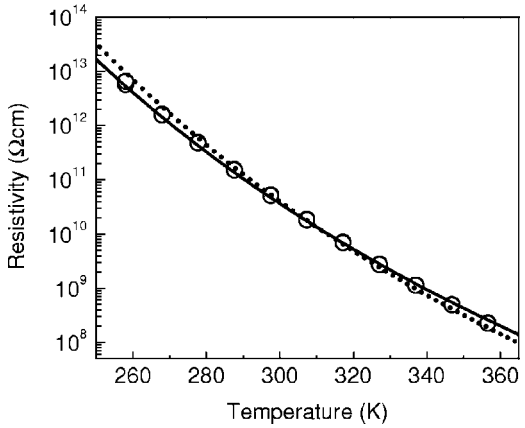

FIG. 4. Illustration of confidence range for $\rho(T)$ fits. Open circles: experimental data from Fig. 3. Straight line: scenario (1) with 20-meV lower effective ionization energy. Dotted line: theoretical behavior of pure (intrinsic) material.

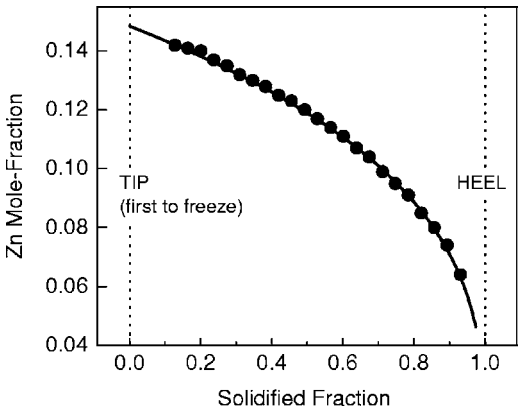

FIG. 5. Measured Zn segregation along the growth axis of a typical gradient-freeze CdZnTe ingot (nominal 10% Zn). Solid circles: experimental data. Solid line: Gulliver-Scheil fit according to Eq. (12) with $k_{Zn}=1.32$.

compensated by a single species of deep acceptors and donors. The Zn mole fraction of this crystal sample was 0.138 and the general material parameters were taken from Ref. 4. The experimental data are actually a double set consisting of a primary and a control resistivity measurement at each temperature.

If the $\rho(T)$ dependence is the only experimental data set to be explained, the absolute deep level defect and net shallow level doping concentrations are of no importance to the fit. In case of a simple three-level model with a deep donor (DD), a shallow acceptor (SA), and a shallow donor (SD) the controlling parameters are the deep level ionization energy and the "overcompensation ratio" $\Phi^0_{D/S}$, which is the ratio of the total deep level concentration to the shallow-shallow compensation offset—e.g.,

$$\Phi^0_{D/S} = \frac{N^{tot}_{DD}}{N^{tot}_{AS} - N^{tot}_{DS}}. \tag{11}$$

Note that the material is semi-insulating for $\Phi^0_{D/S} > +1$.

The following three scenario fits, yielding almost undistinguishable graphs, are shown in Fig. 3: (i) native cation orbital donor with a temperature-independent ionization energy of 0.79 eV and $\Phi^0_{D/S}=7.93$, (ii) native anion orbital acceptor with a temperature-independent ionization energy of 0.79 eV and $\Phi^0_{D/S}=17.0$, and (iii) transition-metal-like donor with a 0/+ transition level, fixed in absolute energy scale at a position corresponding to 0.64 eV below the 296 K conduction-band edge of CdZnTe with 13.8% Zn and $\Phi^0_{D/S}=1.02$.

Of course, all the ambiguity can be removed when additional experimental data are available and included in the same model that will allow to eliminate some of these scenarios. Here, however, we only want to emphasize the fact that one and the same $\rho(T)$ data set can be fitted with different RT ionization energies of the compensating deep level in dependence on the actual nature of the assembly defect states in the sample.

Figure 4 illustrates the sensitivity of such scenario fits to small changes in the effective ionization energy: The straight line corresponds to scenario (i) with a 20 meV lower deep donor ionization energy of 0.77 eV ($\Phi^0_{D/S}=4.13$), which obviously yields a poor fit. Also shown in Fig. 4 is the theoretical temperature dependence for the ideal intrinsic case.

VI. COMPOSITION DEPENDENCE OF IONIZATION ENERGIES

$Cd_{1-x}Zn_xTe$ crystals, grown from the melt by directional solidification, can show a significant Zn segregation from tip (first to freeze) to heel (last to freeze) so that all mole-fraction- (x-) related quantities, especially, the band gap according to Eq. (3), become functions of the axial position in the ingot.

Figure 5 shows an axial Zn concentration profile of a typical $Cd_{1-x}Zn_xTe$ ingot with nominal 10% Zn, grown with the high-pressure electrodynamic gradient-freeze technique at eV Products.[23] The mole-fraction data were obtained from Fourier-transform infrared (FTIR) transmission measurements by comparing the wavelengths at a certain threshold absorption coefficient at the fundamental edge with those of calibration standards.[24] The experimental profile shows a decrease of the Zn concentration from about 14% in the tip to 6% in the heel and can be fitted by Gulliver-Scheil segregation:[25,26]

$$x(z) \propto (1-z)^{k_{Zn}-1}, \tag{12}$$

which may imply complete mixing of the melt and no significant Zn diffusion in the solid (z: solidified fraction). The obtained Zn segregation coefficient is $k_{Zn} \sim 1.32$.

Following the same arguments as for the temperature dependence in Sec. IV, we expect a much stronger composition dependence of the ionization energies of transition-metal-like defects than for defects with shallow, delocalized states. According to Eq. (6), the ionization energies of ideal hydrogenic defects depend primarily on the static dielectric constant of the semiconductor and on the effective masses of the carriers in the respective bands, which may be both compo-

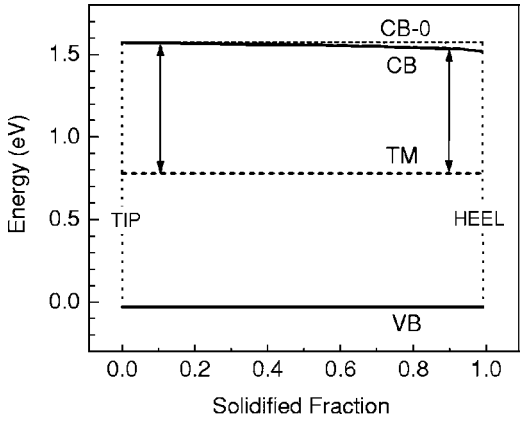

FIG. 6. Absolute energy scale presentation of the axial position dependence of the fundamental RT band edges (CB and VB) and a deep localized donor level (TM) according to the Zn segregation profile from Fig. 5. The deep donor ionization energy decreases from tip to heel (arrows). CB-0: conduction-band edge at tip composition.

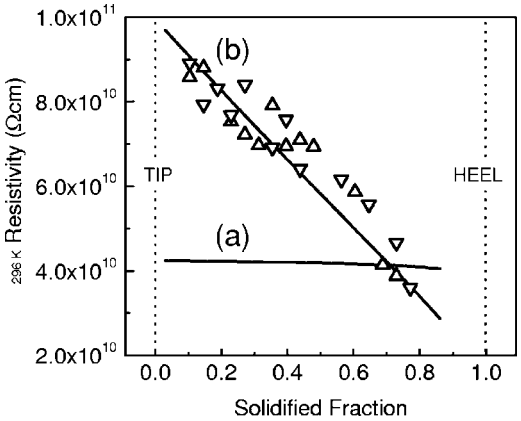

FIG. 7. RT resistivity profile measurement along the growth direction of the CdZnTe ingot from Fig. 5. Up and down tipped triangles: experimental data from Ref. 4 (two adjacent axial rows of test parts). Straight lines: theoretical profiles for (a) composition independent and (b) composition-dependent deep level ionization energies (see Sec. VII for details).

sition dependent. However, the uncertainty in the available experimental data (sometimes already for either of the pure binaries) is usually too large to implement a reasonable correction for the small composition ranges of interest.

Eventually, other effects may influence the ionization energies more dramatically—e.g., spontaneous *AX* or *DX* center formation, which can be caused by energetically favorable configurational deviations of an impurity atom from the ideal substitutional lattice position in dependence on its chemical nature and the composition of the host crystal.[27]

In the following, we keep the shallow level ionization energies independent of the composition but fix the transition metal levels in an absolute scale while shifting the band edge energies $E_V(x)$ and $E_C(x)$ according to the actual composition. For native defects, we proceed the same way as we did for the temperature dependences in Sec. IV; i.e., those that are built up primarily from cation orbitals are assumed to follow the conduction band. Their ionization energies change with the composition if the associated energy levels communicate with the valence band but are composition independent if they generate donor states. The opposite is applied to anion-orbital defects. This "convention" highlights the dramatic effect that the nature of deep level defects can have on the tip-to-heel resistivity profiles.

Figure 6 illustrates the change of the absolute-scale RT band-edge energies from tip to heel of a gradient-freeze-grown CdZnTe ingot according to Eqs. (3)–(5) and the Zn segregation profile from Fig. 5 as a function of the solidified fraction.

VII. TIP-TO-HEEL RESISTIVITY PROFILES

Figure 7 shows an experimental resistivity profile, obtained at RT along the growth direction of the CdZnTe ingot from Fig. 5. Two axial rows of $(5\times5\times2)$ mm^3 test crystals have been cut out from tip to heel. The samples were fabricated into test devices in guard electrode configuration, and a temperature normalized (to 296 K) axial bulk resistivity profile was measured.[4]

Two calculated model profiles are also shown in Fig. 7: Both profiles are obtained from a deep donor compensation model and with the same overcompensation ratio of $\Phi^0_{D/S}=10.1$, constant over the entire crystal length, which corresponds to the ideal case of no segregation of foreign impurities and/or native defects along the growth axis of the single-phase crystal. For curve (a), we assumed a concentration-independent deep donor ionization energy of 0.79 eV (e.g., Cd orbital native defect) and obtained a rather poor match with the experimental profile. In the case of curve (b), the deep donor level is assumed to be generated by a TM-like impurity and has a 0/+ transition level, fixed in absolute energy scale at a position corresponding to 0.79 eV below the 296 K conduction-band edge of CdZnTe with 10% Zn; i.e., the ionization energy is composition dependent and matches the one used for profile (a) only in one point (10% Zn at $z\sim0.71$). Note, however, that even if profile (b) yields a fair fit to the experimental resistivity data, it is not a proof of the TM character of the deep level as the same curve can be generated by tip-to-heel segregation of impurities and/or native defects. Also, the ionization energy used is not a meaningful parameter that can be extracted from a resistivity profile alone as the same fit can be obtained with any ionization energy by appropriately "adjusting" $\Phi^0_{D/S}$.

VIII. SUMMARY

The effect of temperature and composition dependences of deep level ionization energies on electrical compensation has been investigated in the example of the ternary $Cd_{1-x}Zn_xTe$ system. In order to achieve a more realistic interpretation of our experimental results, we implemented a temperature- and composition-dependent definition of the band-edge energies with respect to a host-crystal-independent reference level into the model calculations. The

different, possible relations between the energy states of deep level defects of different nature and the band states are discussed. We demonstrated the dramatic effect of the actual defect nature on the fit results obtained from experimental temperature- and composition-dependent measurements of the electrical bulk resistivity. The potential impact of temperature-dependent ionization energies on high-temperature compensation models has been pointed out.

ACKNOWLEDGMENT

This work has been supported in part by the U.S. Army Armament Research, Development, and Engineering Center (ARDEC) under Contract No. DAAE 30-03-C-1171.

*Corresponding author. Electronic address: mprokesch@ii-vi.com

[1] D. de Nobel, Philips Res. Rep. **14**, 430 (1959).
[2] G. F. Neumark, Mater. Sci. Eng., R. **21**, 1 (1997).
[3] T. E. Schlesinger, J. E. Toney, H. Yoon, E. Y. Lee, B. A. Brunett, L. Franks, and R. B. James, Mater. Sci. Eng., R. **32**, 103 (2001).
[4] M. Prokesch and Cs. Szeles, J. Appl. Phys. **100**, 014503 (2006).
[5] G. F. Neumark, Phys. Rev. B **26**, 2250 (1982).
[6] J. M. Langer and H. Heinrich, Phys. Rev. Lett. **55**, 1414 (1985).
[7] W. Faschinger, J. Cryst. Growth **197**, 557 (1999).
[8] G. D. Watkins, in *Defect Control in Semiconductors*, edited by K. Sumino (Elsevier, Amsterdam, 1990), p. 933.
[9] K. Irmscher and M. Prokesch, Mater. Sci. Eng., B **80**, 168 (2001).
[10] S. Krishnamurthy, A.-B. Chen, A. Sher, and M. van Schilfgaarde, J. Electron. Mater. **24**, 1121 (1995).
[11] W. R. Frensley and H. Kroemer, Phys. Rev. B **16**, 2642 (1977).
[12] B. Späth, J. Fritsche, F. Säuberlich, A. Klein, and W. Jaegermann, Thin Solid Films **480–481**, 204 (2005).
[13] W. A. Harrison and J. Tersoff, J. Vac. Sci. Technol. B **4**, 1068 (1986).
[14] H. Mathieu, A. Chatt, J. Allegre, and J. P. Faurie, Phys. Rev. B **41**, 6082 (1990).
[15] M. Prokesch, K. Irmscher, H. Makino, and T. Yao, Mater. Sci. Semicond. Process. **4**, 601 (2001).
[16] B. K. Meyer and W. Stadler, J. Cryst. Growth **161**, 119 (1996).
[17] C. Wetzel, W. Walukiewicz, E. E. Haller, J. Ager III, I. Grzegory, S. Porowski, and T. Suski, Phys. Rev. B **53**, 1322 (1996).
[18] J. W. Allen, Semicond. Sci. Technol. **10**, 1049 (1995).
[19] S.-H. Wei and S. B. Zhang, Phys. Rev. B **66**, 155211 (2002).
[20] K. H. Chow and G. D. Watkins, Phys. Rev. B **60**, 8628 (1999).
[21] G. D. Watkins, J. Cryst. Growth **159**, 338 (1996).
[22] J. A. van Vechten, in *Handbook on Semiconductors III*, edited by S. P. Keller (North-Holland, Amsterdam 1980).
[23] Cs. Szeles, S. E. Cameron, S. A. Soldner, J.-O. Ndap, and M. D. Reed, J. Electron. Mater. **33**, 742 (2004).
[24] FTIR measurements and mole-fraction conversion by J.-O. Ndap, eV Products, 2005.
[25] G. H. Gulliver, J. Inst. Met. **9**, 120 (1913).
[26] E. Scheil, Z. Metallkd. **34**, 70 (1942).
[27] D. J. Chadi and C. H. Park, Mater. Sci. Forum **196–201**, 285 (1995).